CrossMark

ORIGINAL PAPER - EXPLORATION GEOPHYSICS

Petrophysical evaluation of well log data and rock physics modeling for characterization of Eocene reservoir in Chandmari oil field of Assam-Arakan basin, India

Mithilesh Kumar[1] · R. Dasgupta[1] · Dip Kumar Singha[2] · N. P. Singh[2]

Abstract Petrophysical evaluation of well log data has always been crucial for identification and assessment of hydrocarbon bearing zones. In present paper, petrophysical evaluation of well log data from cluster of six wells in the study area is carried out in combination with rock physics modeling for qualitative and quantitative characterization of Eocene reservoir in Chandmari oil field of Assam-Arakan basin, India. Petrophysical evaluation has provided the estimation of fluid and mineral types, rock/pore fabric type and fluid and mineral volumes for invaded and virgin zones. Calibrations are made where core data were available. Rock physics study is carried out for analyzing the influence of porosity, mineral compositions and saturation variations on the elastic properties of the subsurface. The rock physics modeling allowed quantitative prediction of relationship between porosity, saturation (gas, oil and water), clay volume and the elastic properties. Cross-plots of different elastic parameters are generated to identify the lithology variability and pore-fluid type, and to establish likely distinction between the hydrocarbon bearing sands, brine sands and shale. The Eocene reservoirs are found to be primarily sandstone intermixed with incidental clay matrix and some calcareous cementation. Sands are interpreted to be continuous in most of the blocks. The effective porosity for these sands varies from 15 to 22% in most of the wells. A wide range of variation is observed in water saturation with lowest being 5%. Finally, a numerical rock physics model is prepared to predict the elastic properties of the rock from petrophysical properties.

Introduction

Superior quality well log data are essential for the high-quality seismic reservoir characterization because well log data are routinely used for wavelet estimation, low frequency model building, seismic velocity calibration, and time-to-depth conversion. Well logging plays a crucial role in the determination of the production potential of a hydrocarbon reservoir (Ellis 1987). Several authors namely, Joshi et al. (2004), Neog and Borah (2000), Ishwar and Bhardwaj (2013), have shown the relation of different petrophysical parameters with the reservoir characterization and production, and hence reduced the uncertainty of reservoir evolution in Upper Assam basin. The petrophysical evaluation of log and core data provides main properties such as lithology, porosity, clay volume, grain size, water saturation, permeability and many others, which are essential for the evaluation of the reservoir formation (Rider 1996; Mukerji et al. 2001; Sarasty and Stewart 2003). Though, the prediction of such properties is complex, as the measurement sites available are sparsely located. The conventional method used for the identification of litho-facies is by the direct observation of underground cores (Chang et al. 2002). Determination of lithology by direct observation from core data are, however, more accurate, but the analysis process is an expensive and lengthy task and not always reliable. On other hand, the core data information available at certain

✉ N. P. Singh
 singhnpbhu@yahoo.co.in

1 Oil India Limited, Duliajan, Assam 786 602, India

2 Department of Geophysics, Institute of Sciences, Banaras Hindu University, Varanasi, Uttar-Pradesh 221 005, India

مدينة الملك عبدالعزيز
للعلوم والتقنية KACST

 Springer

intervals is used as the basis to establish an interpretation model for other zones with similar log responses. Therefore, in order to perform reliable petrophysical properties estimation, initial preprocessing on raw data is required before log analysis. The preprocessing stage normally employed is meant for the correction of environmental effects, indication of spatial minerals, correction of resistivity logs and so on (Rider 1996). For multi-well analysis, further preprocessing such as recalibration of logs is also required. In this study, Gamma Ray logs, Neutron logs, Density logs, Deep resistivity logs and shallow resistivity logs are recognized as lithology logs.

Rock physics models relate the link between reservoir parameters such as: porosity, clay content, sorting, lithology, water saturation and seismic properties, namely; ratio of P-wave velocity (V_p) to S-wave velocity (V_s), density and elastic moduli (Avseth et al. 2005; Datta Gupta et al. 2012). Petrophysical interpretation of well log data and rock physics modeling provides a framework for the interpretation of seismically derived elastic property volumes (Mavko et al. 1998; Gray et al. 2015). Hence, logs are required for petrophysical interpretation and subsequent rock physics modeling for calibration of elastic logs (Density, P-sonic, and often S-sonic logs) that are consistent through inter-and intra-well covering the entire vertical interval of interest. It is often the case that the well log data do not satisfy these criteria due to various reasons namely different tool measurements, different borehole environments, different borehole fluids, poor quality logging conditions, invasion of borehole fluids into the formations, alteration of the formation properties due the presence of borehole fluids and missing recorded data etc. Thus, the well log data need to be conditioned, corrected and synthesized to provide complete and reliable input for reservoir characterization study. Therefore, the missing data have been synthesized to provide a complete set of elastic logs for the interval of interest for all the wells.

The Upper Assam Basin where hydrocarbon exploration and production is in progress since last few decades has gradually assumed the status of a matured oil and gas producing province (Naidu and Panda 1997). However, there is possibility of a lot of bypassed reservoirs which could still be identified from this old oilfield using latest approaches. The present study is intended to make available the petrophysical properties, as measured by well logs in the study area and to explore empirical relationships between petrophysical properties and various parameters. The main objective of the study is to evaluate the hydrocarbon potential in the field by petrophysical analysis and inference, as well as rock physics analysis for better understanding of physical properties of the reservoir and creating new exploration and development opportunities in the field.

Study area

The study area is Chandmari oil field which is a part of petroliferous sedimentary Assam-Arakan basin situated in north eastern part of India (Fig. 1). This field comes under Upper Assam Shelf having 7000-m-thick sediments which is one of the major tectonic elements of the basin. Sedimentary sequences ranging in age from Late Mesozoic to Cenozoic are exposed in the Assam-Arakan Basin (Balan et al. 1997; Mandal and Dasgupta 2013). In Upper Assam Shelf, the main reservoir rocks are the Sylhet Formation limestones (Eocene), Kopili Formation interbedded sandstones (Late Eocene - Oligocene), Tura (basal) marine sandstones and Surma Group alluvial sandstone reservoirs (Mandal and Dasgupta 2013). The most productive reservoirs are the Barail (Oligocene- Miocene) main pay sands and the Tipam Group (Miocene) massive sandstones. Other formations are Girujan (Miocene), Namsang (Pliocene) and Siwalik/Dhekiajuli (Recent) (Balan et al. 1997; Wandrey 2004; Mandal and Dasgupta 2013). The sequences can be divided into shelf facies and basinal (geosynclinal) facies. The area has been discovered earlier through the use of 2D seismic and has proven reserves from clastic reservoirs at two depth levels. The target sandstone reservoir of this oil field is of the Eocene age.

Well log data analysis

Log data available

Total six wells having various conventional log responses are available in the study area. The availability of different log data is tabulated in Table 1.

After loading and checking of log data, it was found that most of the wells are aligned in depth and does not require any depth shift. However, on analyzing all the raw well data, it was observed that most of the wells have high differential caliper reading which may affect the quality of the logs. Especially the padded tools may suffer from poor pad contact and hence may give poor quality data. One way to understand the effect of this borehole caving is to cross plot the recorded data taking differential caliper (DFCAL) in the third axis. Moreover, the effects of tool current fluctuation, irregular tool tension, cycle skipping have been understood by careful observation of log plots and cross-plots. For data quality check (QC) and to identify the potential bad data points, cross-plots of density (RHOB) versus neutron porosity (NPHI) colored by differential caliper and RHOB versus transit travel time (DT) colored by differential caliper in one representative well-A are shown in Figs. 2 and 3, respectively.
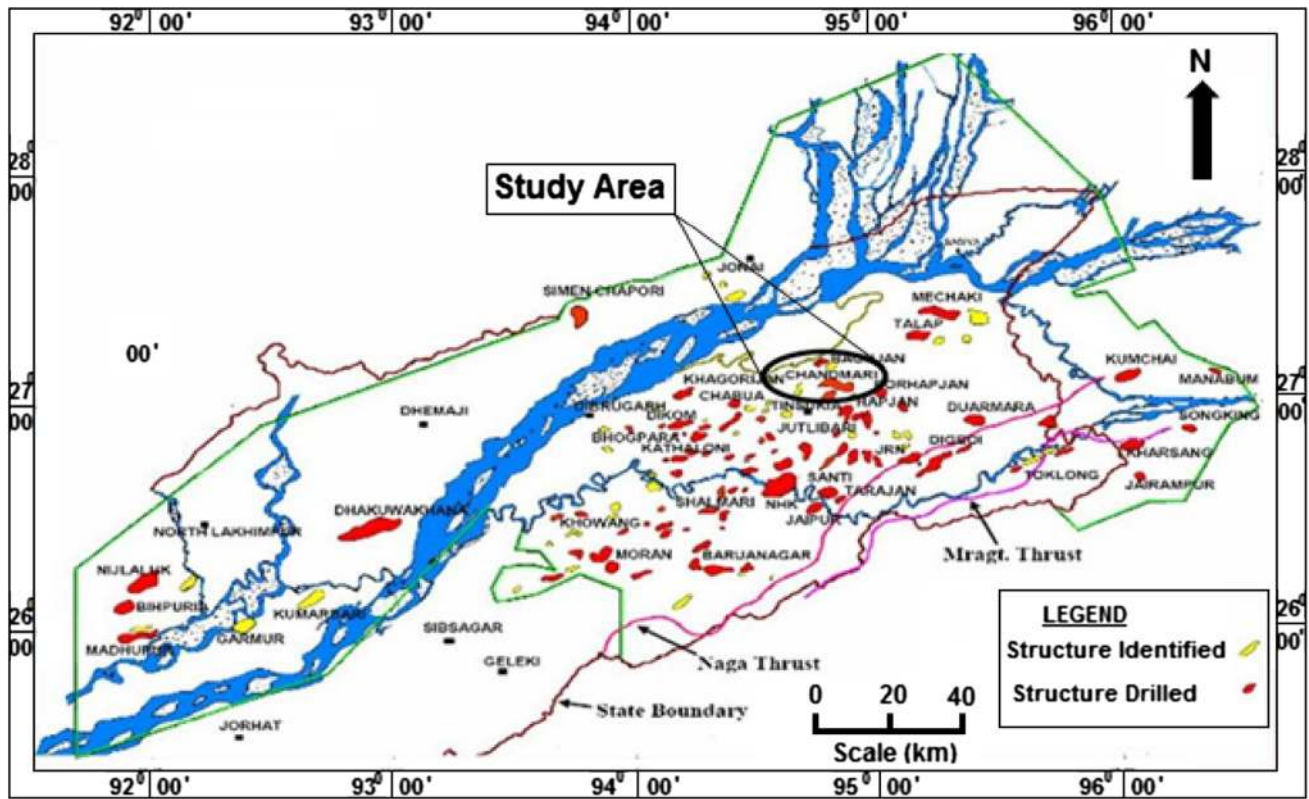
Fig. 1 Location map of study area in Upper Assam Shelf (after Mandal and Dasgupta 2013)

Table 1 Availability and non-availability of conventional log data of six wells

Well name	GR	SP	Caliper	Deep resistivity	Shallow resistivity	Micro resistivity	Density	Neutron porosity	PEF	DRHO	P-Sonic	S-Sonic
A	√	√	√	√	√	√	√	√	√	X	√	√
B	√	√	√	√	√	√	√	√	√	√	√	√
C	√	√	√	√	√	√	√	√	X	√	X	X
D	√	N	√	√	√	√	√	√	X	√	√	√
E	√	√	√	√	√	√	√	√	√	√	X	X
F	√	√	√	√	√	√	√	√	√	X	√	X

√: Availability of data, X: non-availability of data, *GR* Gamma Ray, *SP* Spontaneous, *PEF* Photoelectric, DRHO: Density

From the cross-plots, it is noticed that there are effects of bad borehole in the logs. There are some data points which fall outside the main trend and have high differential caliper (DFCAL). Similar plots are made for all other wells used in the study to identify potential bad data points.

Log conditioning

Log conditioning is the final stage in preparation of log data for petrophysical evaluation, in which poor quality data are identified and are replaced by synthesized data. In particular, the key logs for petrophysical evaluation are conditioned. Figure 4 illustrates how the poor quality data in density log are synthesized using other logs. The solution is achieved by synthesizing a density log through multiple linear regressions from other log curves. The regression formula is obtained by running regression analysis for all wells in zones where the density log is considered to be of good quality. The synthetic density curve is then compared with the measured density log. The measured curve is replaced by the synthesized curve where the later is determined to be more representative of the in situ rock density. The conditioning is an important

Fig. 2 RHOB versus NPHI cross-plot colored by differential caliper (data falling within the marked *circle* represent bad data)
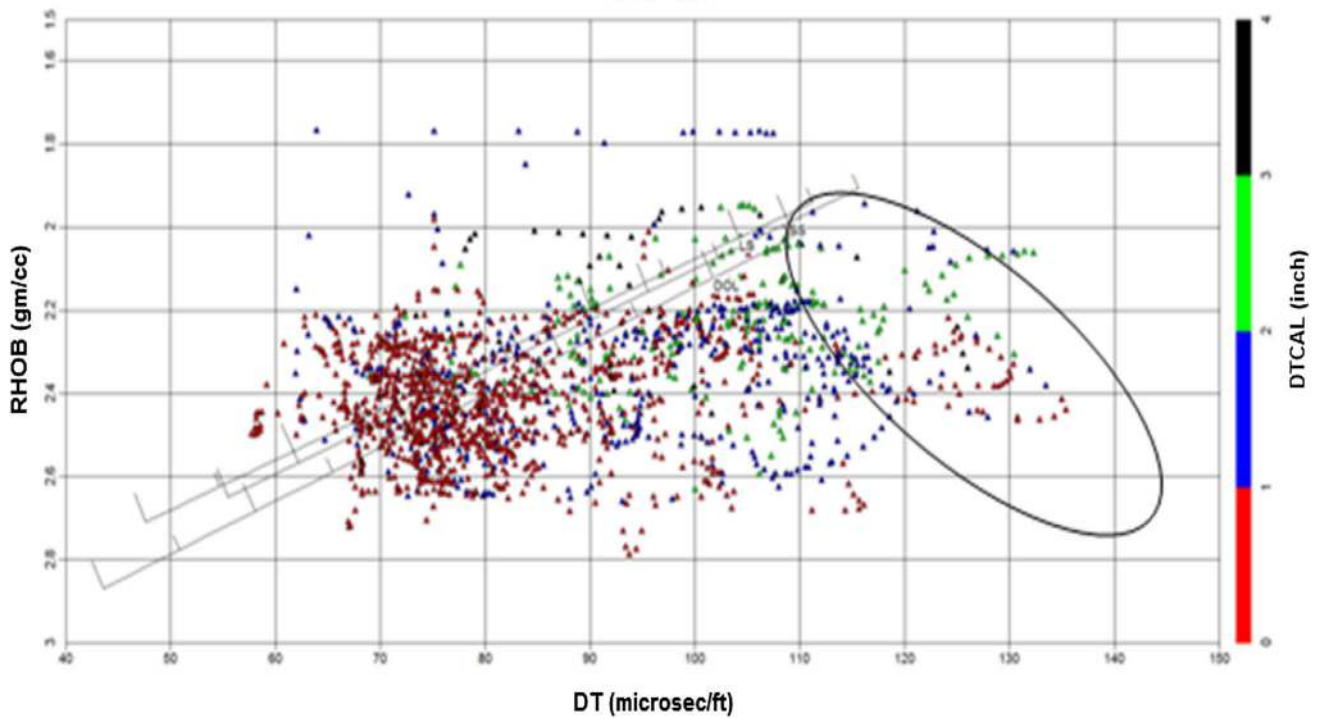

Fig. 3 Cross-plot between RHOB and DT colored by differential caliper (data falling within the marked *circle* represent erroneous data)

process as the derived porosity and volume of clay as well as the rock physics analysis is strongly dependent on the density log. Several iterations are required to produce a log that is consistent with rock physics model and sonic log data. The process of density conditioning is illustrated below for a representative well-A.
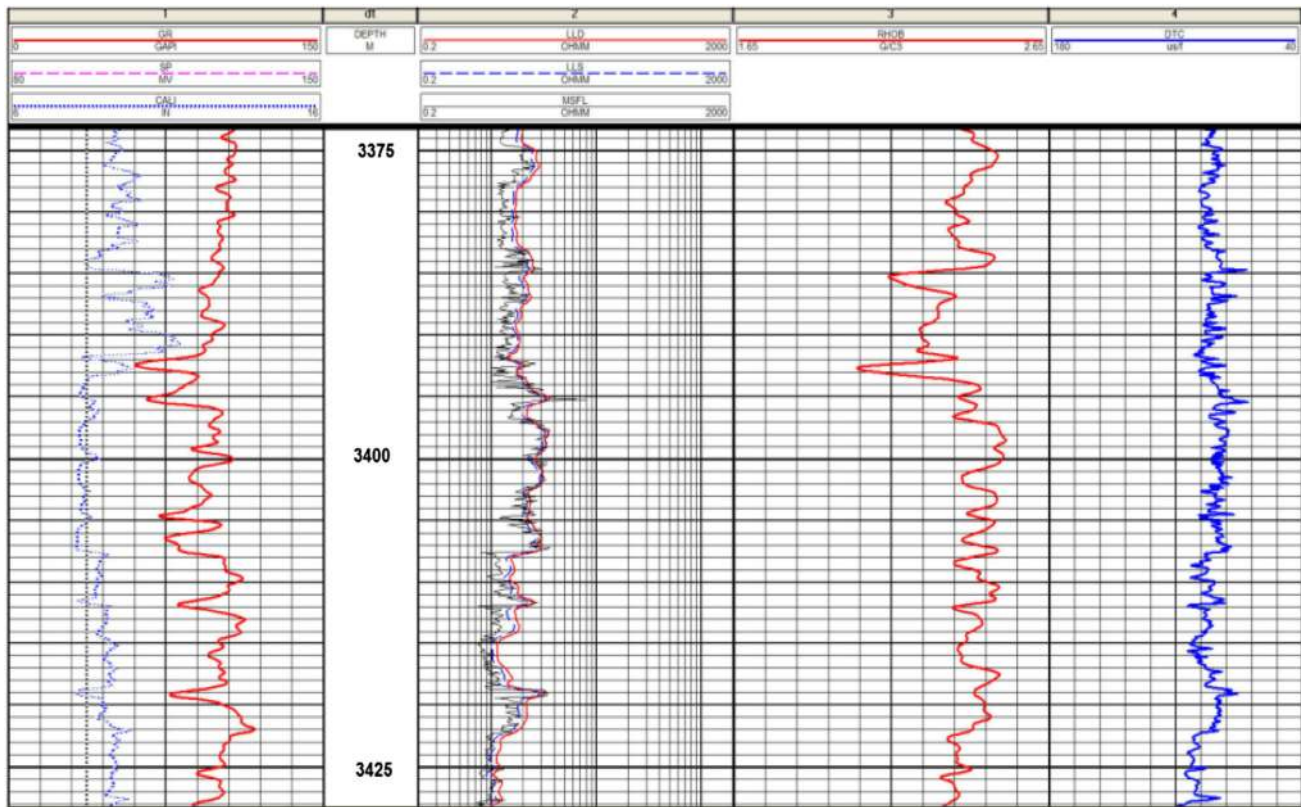
Fig. 4 Measured density curve on track-3 (*red*) for well- A requires conditioning

Curve synthesis and reconstruction

The objective of curve synthesis and reconstruction is to condition the logging data at wash-out intervals, missing sections or where the data are obviously incorrect. In example the density curve was conditioned at bad-hole interval (Figs. 4, 5) by curve synthesis and reconstruction using data from the closest interval with good borehole conditions.

In Fig. 4, track-3, the red curve is the measured density data in which some poor quality data are observed against the wash-out section. The synthetic density curves are generated for this interval using the multi-linear regression equation established using deep resistivity (LLD) and DT data in the interval 3393–3420 m.

The log plot in Fig. 4 shows higher values of the caliper reading in the interval 3385–3393 m. The measured data in this interval may be affected by the bad hole. However, hole is good in the interval 3393–3420 m. Hence, measured data in this interval is suitable to establish regression relation of density with other available curves and thereby in construction of a synthetic density curve. In this case, deep resistivity and P-sonic showed a good correlation with the measured density and have been used to synthesize the density curve.

The log plot in Fig. 5 confirms that the synthesized density log is reliable. It shows a good match with the

measured data over the good-hole section and hence can be used to replace density data against the bad-hole section where the measured data is bad. Thus, the measured density was replaced by the synthesized density data in the interval 3385–3393 m. The same technique is applied to condition measured density, P-sonic and neutron porosity curves for all the wells used in this study where the data quality were poor or there were data gaps.

Cross-plot analysis for quality control (QC) of conditioned log data

The corrected and conditioned data must be confirmed through quality control methods in order to guarantee the reliability of the correction and conditioning. Therefore, in this study, required cross-plots have been used to carry out the quality control of the conditioned data. Figures 6 and 7 depict neutron versus density cross-plot and density versus P-sonic cross-plot of the raw (colored in blue) and conditioned (colored in red) data for well-A. From these figures, it is clear that the conditioning has helped to bring the scattered data outside the main trend back into the main trend. However, there are some suspicious data trends still remaining in density versus neutron plot which are supposed to be coming from coal zone. To synthesize these
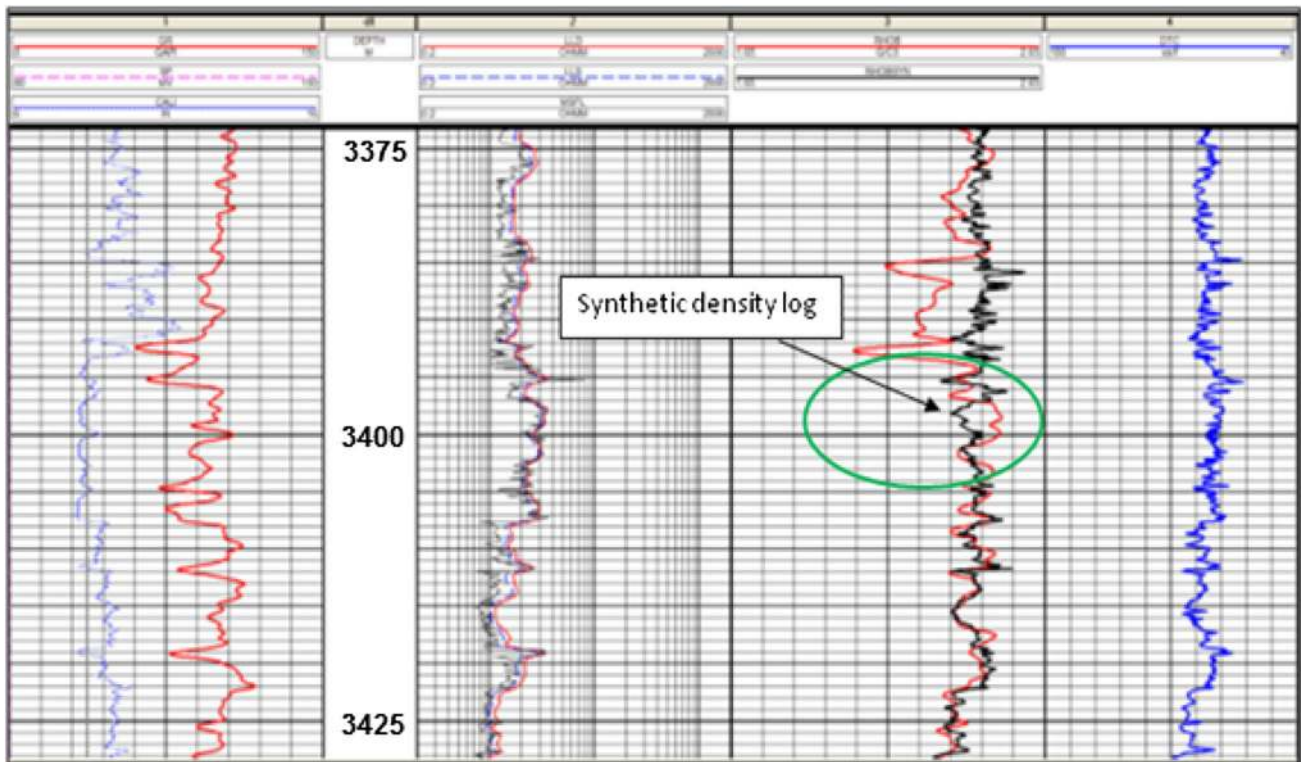
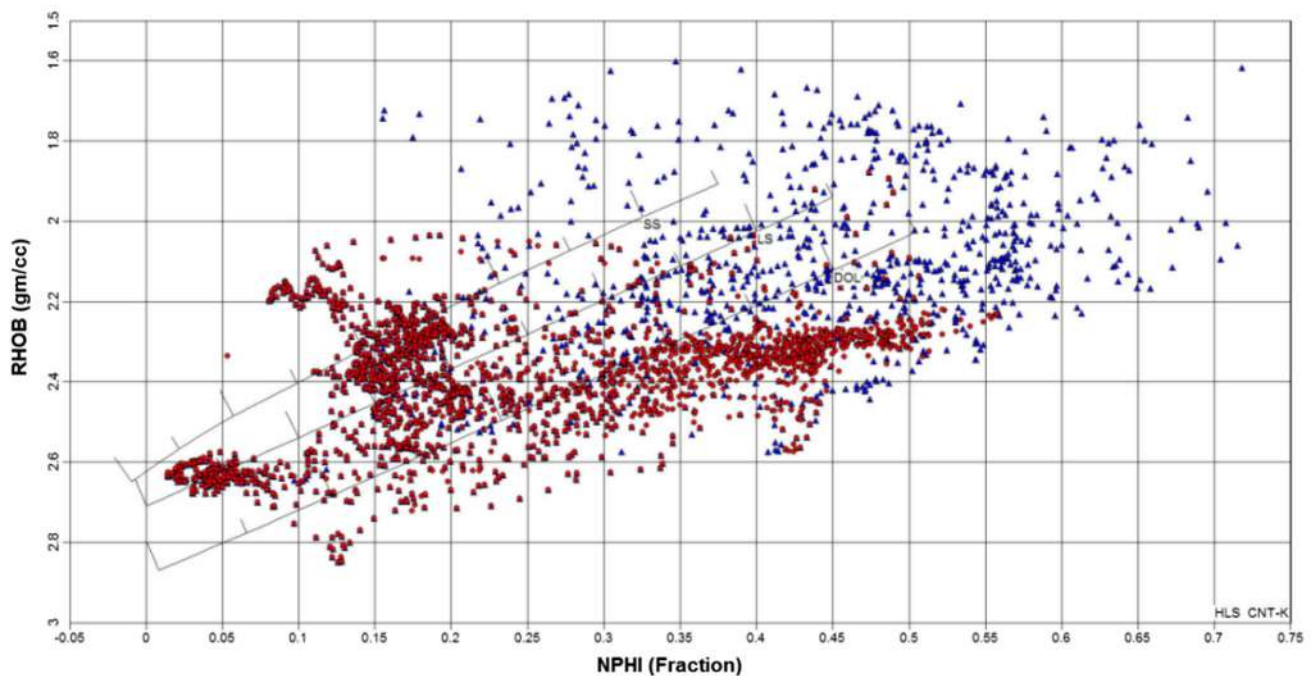**Fig. 5** Well A-synthesized density curve (*black*) on top of measured density curve

Fig. 6 Well A is conditioned by RHOB and NPHI (*red*) on top of measured RHOB-NPHI (*blue*)

data, there should be some good quality data available from a similar coal zone in and around the bad data zone. In this case there is no such zone available and hence for this zone curve synthesis was not possible.

Another important criterion for rock physics modeling is that input well data has to be consistent from well to well unless there is significant geological variation. Since, without consistent input log data, it is not possible to
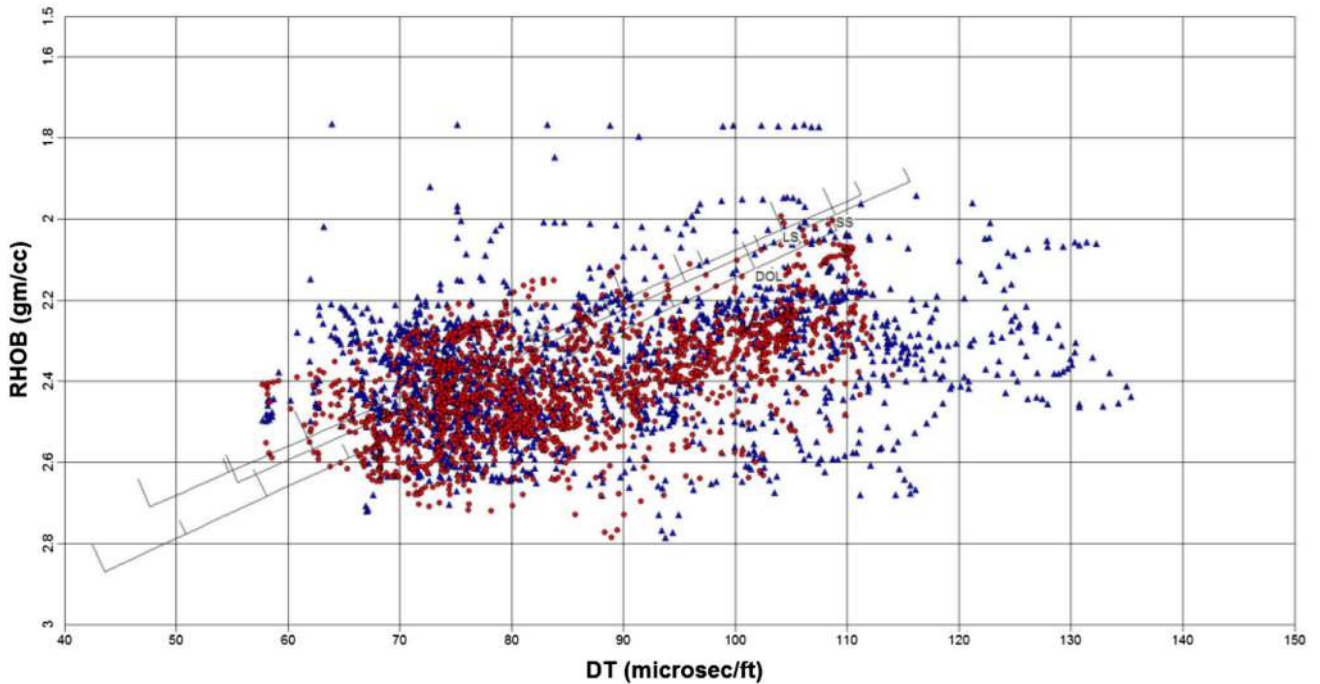
Fig. 7 Well A is conditioned by RHOB and DT (*red*) on top of measured RHOB-DT (*blue*)

establish a consistent rock physics model. Therefore, the consistency of the well data is tested by cross-plotting all well data on top of each other as shown in Figs. 8 and 9 where different color points in plot represent data from different wells.

From above cross-plot analysis (Figs. 8, 9), it is clear that the conditioned data are consistent, as the data from all the wells are following the same trend in the cross-plots. Hence, no normalization is required for using this data as input to petrophysics and rock physics studies.
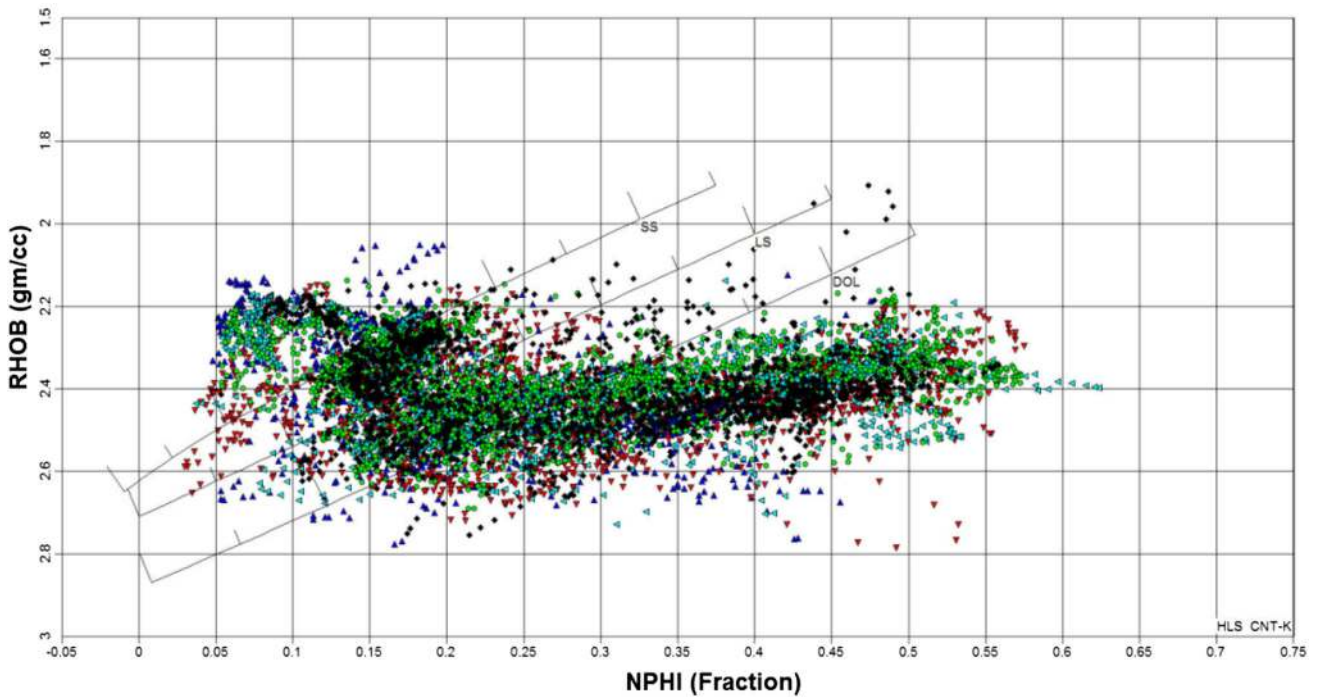

Fig. 8 Multi-well conditioned RHOB versus NPHI cross-plot to test the consistency of data
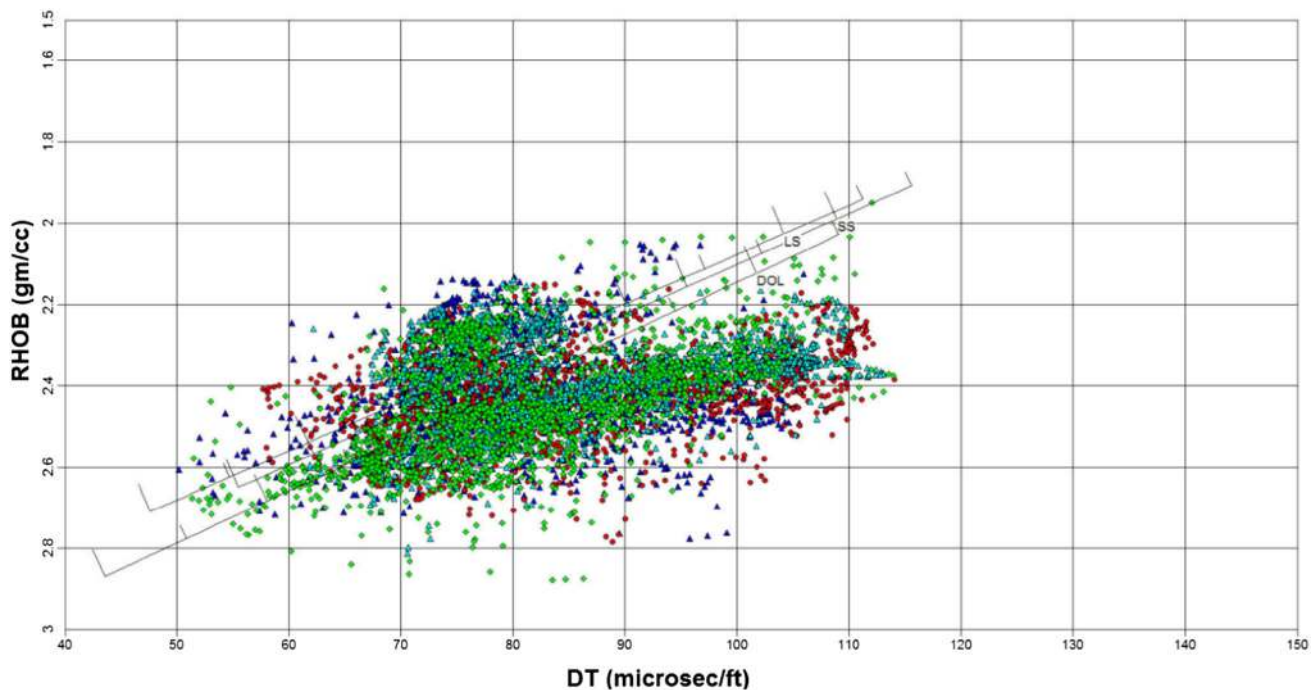
Fig. 9 Multi-well conditioned RHOB versus DT cross-plot to test consistency of data

Petrophysical analysis

Petrophysical analysis deals with the properties of porous media such as: porosity, permeability, water saturation, fluid identification, resistivity, shalyness particularly in reservoir rock and contained fluids (Inichinbia et al. 2014). These properties and their relationship are generally used to identify and assess reservoir rock, source rock and cap rock. The petrophysical analysis provides suitable input to the rock physics studies and meaningful evaluation of petrophysical properties of the reservoir rocks. The petrophysical evaluation consists of estimation of the volumes of minerals and fluids present in the invaded and virgin zones. The volume of clay is first estimated using a combination of Gamma ray (GR) and Neutron-density logs. Complex lithology method has been employed for mineral analysis, porosity and saturation estimation in all the wells. Neutron-density log for porosity calculation and the deep resistivity log for water saturation are used for all the zones.

Lithology determination

The main lithology of the reservoir in this field is shaly sandstone with quartz being the major mineral. Volume of clay layer (VCL) is computed from GR or a combination of GR and RHOB-NPHI. When a combination of different clay indicator is used, an independent calculation of clay volume (say VCLGR and VCLND) is made for each clay

indicator and the final clay volume at each depth is the minimum clay volume for the specified indicators where the two VCL curves track each other within a tolerance limit. The places where the two curves do not track each other, the final judgment on acceptance of a curve is made on the basis of other supporting clay volume indicator like SP, resistivity, P-sonic, V_P/V_S etc.

Volume of clay from gamma log (VCLGR)

The volume of Clay from GR (VCLGR) is computed using the following equation.

$$VCLGR = 0.0006078 * (100 * I)^{1.58527} \quad \text{for } I \leq 0.55$$
$$VCLGR = 2.1212 * I - 0.81667 \quad \text{for } 0.55 < I < 0.73$$
$$VCLGR = I \quad \text{for } I \geq 0.73$$

$$(1)$$

where $I = (GR_{log} - GR_{clean})/(GR_{clay} - GR_{clean})$.

The clay volume responses from GR computed by the different methods are shown in Fig. 10.

Volume of clay from neutron-density cross-plot (VCLND)

VCL from RHOB and NPHI cross-plot is computed using an equation of a clean line (Dresser 1981) which is defined by two points on the sand line and a clay point (Fig. 11).

The clean points define the clean line (VCL = 0). The clay line (VCL = 1) runs parallel to the clean line and
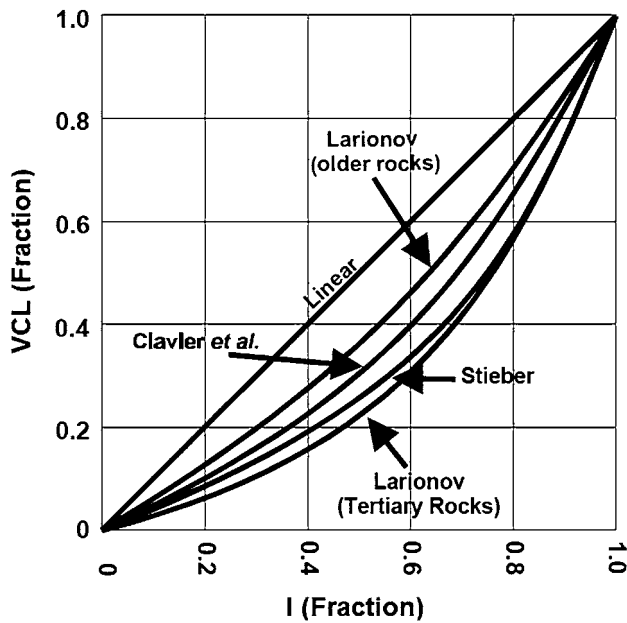
Fig. 10 VCL responses from GR computed by different methods

passes through the clay point. Lines of constant VCL run parallel to those lines at a position proportional to the relative distance between the clean and clay lines, as shown in Fig. 11. The 'end points' in density, neutron and gamma ray for wet clay are chosen such that the volume of wet clay is estimated to be around 70–75% against shale section. On the basis of available data, petrophysical analysis and rock physics modeling, the VCL from neutron-density cross-plot and GR allowed the identification of reservoir rock and non-reservoir rock more clearly in most of the zones and provided greater consistency between the petrophysical and rock physics models.
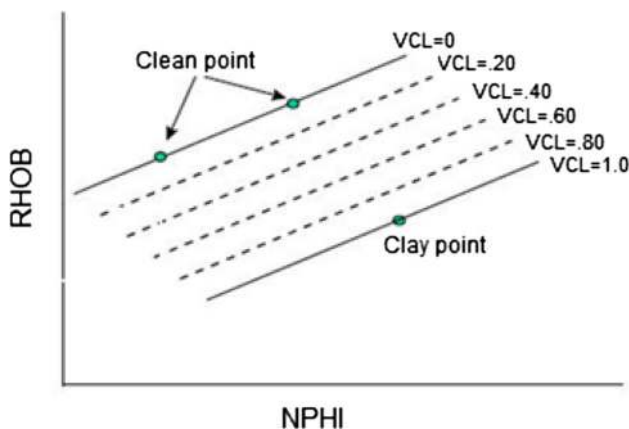

Fig. 11 Schematic diagram of volume of clay from density and neutron cross-plot

Computation of PHIE and water saturation (S_w) by complex lithology model

Porosity is calculated with the 'Multimin' method using the density and neutron logs. The clay end points used for porosity calculation are the same as the end points used in VCL calculations. Figure 12 shows the rock model based on the 'effective porosity and wet clay.'

The effective porosity is computed from neutron-density cross-plot (Bateman 1985).

$$\phi_e = \frac{\phi_D \times \phi_{N_{sh}} - \phi_N \times \phi_{D_{sh}}}{\phi_{N_{sh}} - \phi_{D_{sh}}} \qquad (2)$$

where ϕ_e is the effective porosity, ϕ_D is the density porosity, $\phi_{N_{sh}}$ is neutron porosity of shale, ϕ_N is neutron porosity, $\phi_{D_{sh}}$ is the density porosity of shale.

The porosities ϕ_D and ϕ_N in Eq. (2) have been corrected for the effect of residual hydrocarbon before dealing with the equations.

The density derived porosity ϕ_D is corrected using the residual hydrocarbons by the formula,

$$\phi_D = \left[\delta_{ma} - \delta + 1.07\left(\frac{R_{mf}}{R_{xo}}\right)^{1/2}(1.11 - 1.24\delta_h)\right] \Big/ \{\delta_{ma} - 1 + 1.07(1.11 - 1.24\delta_h)\} \qquad (3)$$

where δ_{ma} is matrix density, δ is the log reading, δ_h is the hydrocarbon density, R_{mf} is the mud filtrate resistivity, R_{xo} is the flushed zone resistivity, and ϕ_D is the residual hydrocarbon corrected porosity (Schlumberger 1967).

The neutron derived porosity ϕ_N is corrected using the residual hydrocarbon by the formula

$$\phi_N = \phi_{na}/[(1 - S_{hr})\{(\delta_{mf}(1 - P) - \delta_h - 0.3)/\delta_{mf}(1 - P)\}] \qquad (4)$$

where ϕ_{na} is the apparent neutron porosity, P is the mud filtrate salinity (10^6 ppm), and ϕ_N is the neutron porosity corrected from hydrocarbon effect (Dresser 1981).

Water saturation in shaly sand is determined using Poupon–Leveaux Indonesian model (Poupon and Leveaux 1971). Indonesian equation is defined as
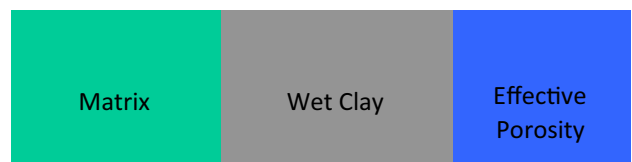

Fig. 12 The display of 'effective porosity and wet clay' model

$$\frac{1}{R_t} = S_w^n \left[\left(\frac{V_{sh}^{2-V_{sh}}}{R_{sh}} \right)^{1/2} + \left(\frac{\phi_e^m}{R_w} \right)^{1/2} \right]^2 \qquad (5)$$

$$S_w = \left\{ \left[\left(\frac{V_{sh}^{2-V_{sh}}}{R_{sh}} \right)^{1/2} + \left(\frac{\phi_e^m}{R_w} \right)^{1/2} \right]^2 R_t \right\}^{-1/n} \qquad (6)$$

where ϕ_e = Effective porosity, V_{sh} = Shale volume, R_{sh} = Resistivity of shale, R_w = Water resistivity, R_t = Deep resistivity, S_w = Water saturation.

The clay end points used for porosity calculation are the same as the end points used in VCL calculations. For iterative hydrocarbon correction, residual hydrocarbon saturation S_{rh} is derived from S_{xo} or from an empirical equation that uses S_w.

We used the Poupon–Gaymard equations (Gaymard and Poupon 1968) for residual hydrocarbon corrections to the neutron and density to resolve porosity and lithology through an iterative technique. The complex lithology neutron-density model for mineral analysis, porosity estimation and saturation calculation is shown in Fig. 13.

The Pickett plot analysis (Figs. 14, 15) enabled us to determine R_w for the reservoir sand.

From two cross-plots (Figs. 14, 15), it is clear that a value of 0.45–0.50 Ωm at borehole temperature (BHT) can be taken as R_w to estimate S_w from Indonesian equation. The relevant parameters used in estimating water saturation are given in Table 2.

Petrophysical results

The final petrophysical results of one representative well are shown in Fig. 16. These results are based on above method and current data available. The raw and conditioned logging curves are shown at tracks 1–4 in Fig. 16. The results of petrophysical analysis are shown in track 5 and 6. The track 5 shows volume of wet clay (shaded gray), volume of mineral quartz (shaded yellow) and effective porosity (shaded cyan), while track 6 represents effective water saturation (shaded red).

The computed mineral volumes and fluids are used to find out the best quality reservoir sands. On the basis of VCL, S_w and PHIE, the best quality reservoirs identified are listed in Table 3 for representative well-A. Similarly, we have identified reservoir sands in other wells used in this study.
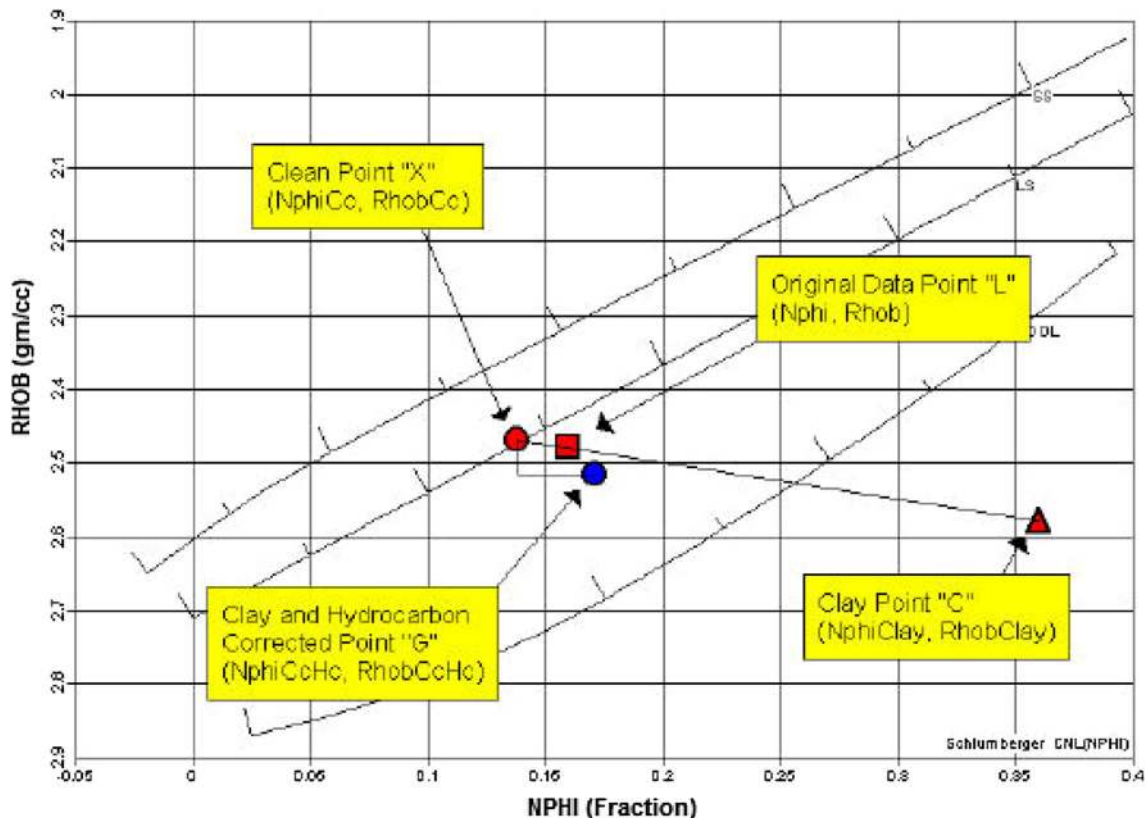

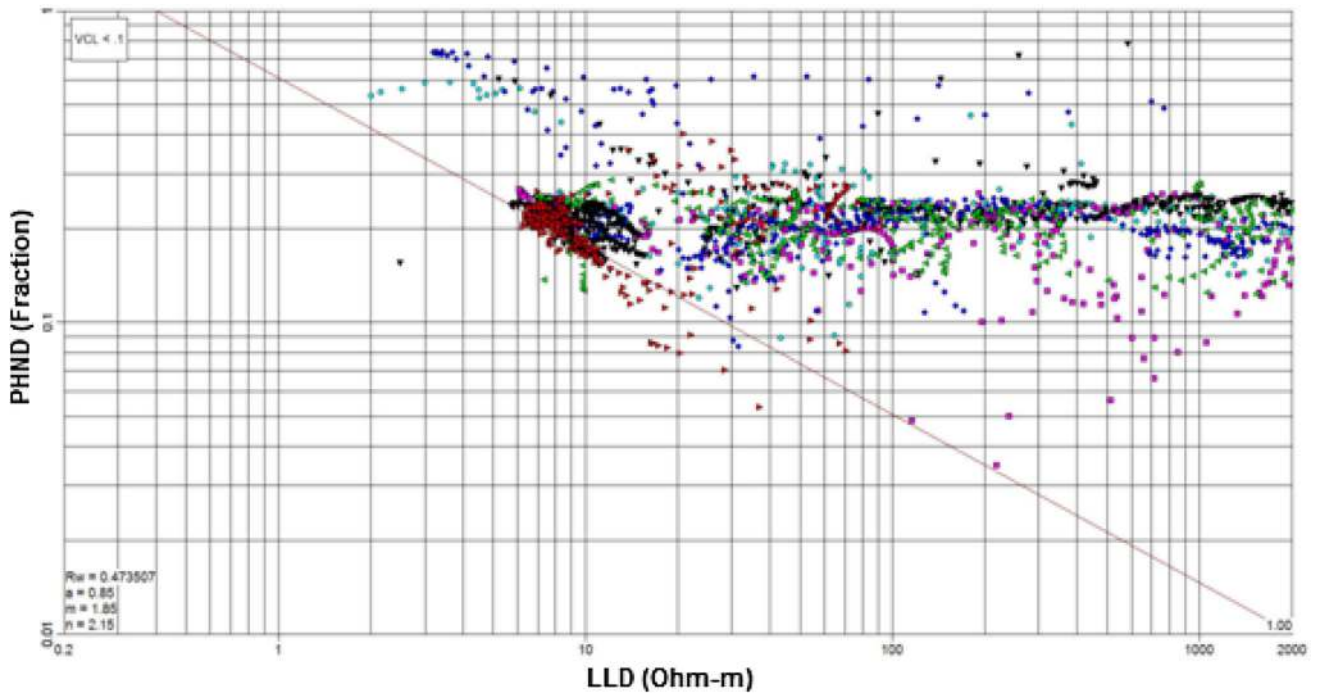Fig. 13 Simple diagram of complex lithology neutron-density model

Fig. 14 Multi-well Pickett plot between PHID (density porosity) and LLD (deep resistivity) for determining R_w
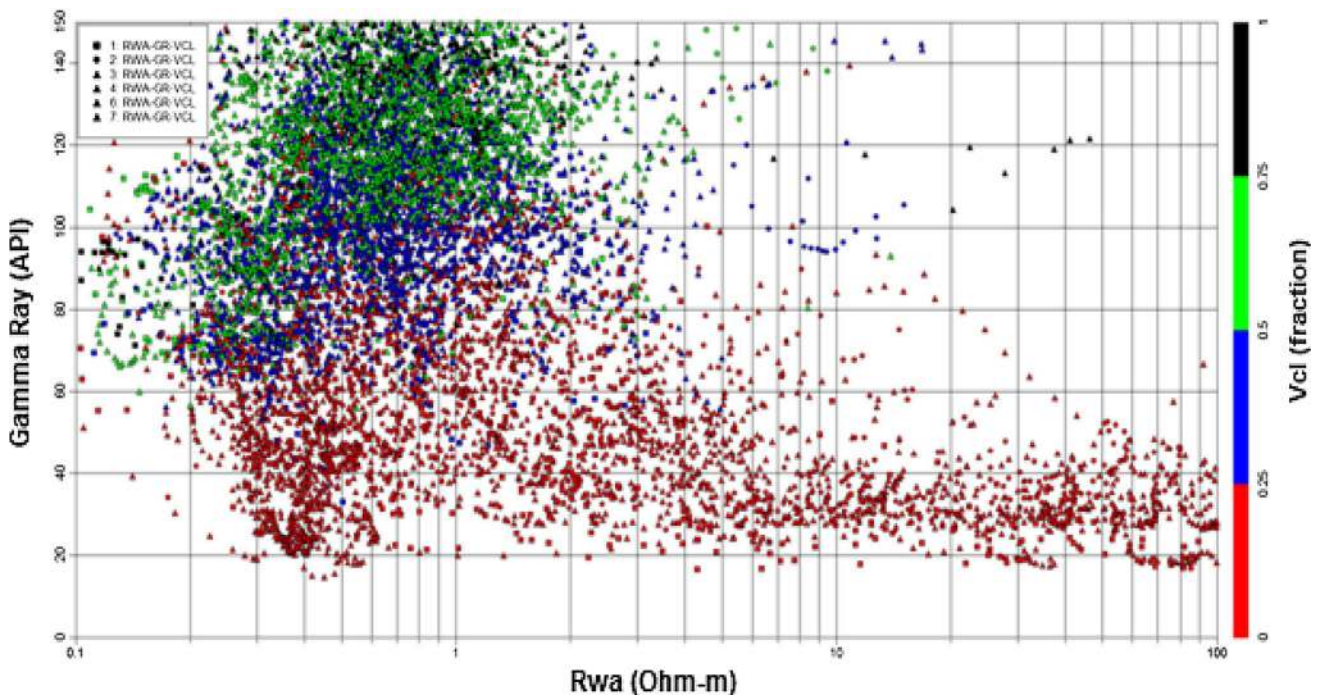

Fig. 15 Multi-well GR versus RWA plot to determine R_w

Rock physics modeling

The rock physics studies have allowed combining elastic properties of minerals and fluids that predict the measured elastic logs of the rocks: density, P-velocity and S-velocity (Avseth et al. 2005; Xin and Han 2009). The analysis confirms that the rock physics model devised for these logs is appropriate to explain the rock behavior, understand the relationships between the petrophysical and elastic rock properties and it could synthesize good quality P-sonic and

Table 2 Parameters used for determining water saturation

Parameter	Value
R_W	0.45–0.50 Ωm @BHT
m	1.85
n	2
a	0.9
R_{tcl}	5 Ωm
R_{xocl}	5 Ωm

Table 3 Reservoir parameters estimated for representative well-A

Interval (m)	VCL (%)	S_w (%)	PHIE (%)
3926.3–3927.4	15–20	28	20
3901.4–3905.6	5–15	19–25	20–35
3848–3850.4	5–10	20–22	35

S-sonic log where no recorded sonic logs were available (Mavko and Mukerji 1995; Avseth et al. 2006).

The modeling was started with a shale density of 2.8 g/cc. This led to a systematic error in P-wave velocity. This error was fed back to find the best effective clay density to obtain a good fit to the P-velocity. A plot of clay density versus depth gave a systematic variation, and a curve was fitted for the interval below Lk + Th. These curves were then used as clay density. The aspect ratio of clean and S-velocity of clay were then optimized to fit the data with measured shear wave velocity. Thereafter, V_P/V_S of clay was adjusted to optimize the fit to the measured P-velocity. The model in this case is based on the volume of clay and saturation derived from the petrophysics and the total porosity derived from the density. The derivation of model involved mixing of minerals and pore space, then the fluids and finally the fluid mixture is introduced into the porous mineral mix via Gassmann's equations (Batzle and Wang 1992; Mavko and Mukerji 1995; Mavko et al. 1998; Berryman 1999; Han and Batzle 2004). The modeling started under the assumption that the measured data are representative of invaded formation. The saturation is set to $S_W^{0.2}$ to model the invaded zone for all the wells. Other fluids can also be introduced to understand the sensitivity of the rock properties to the fluid type.
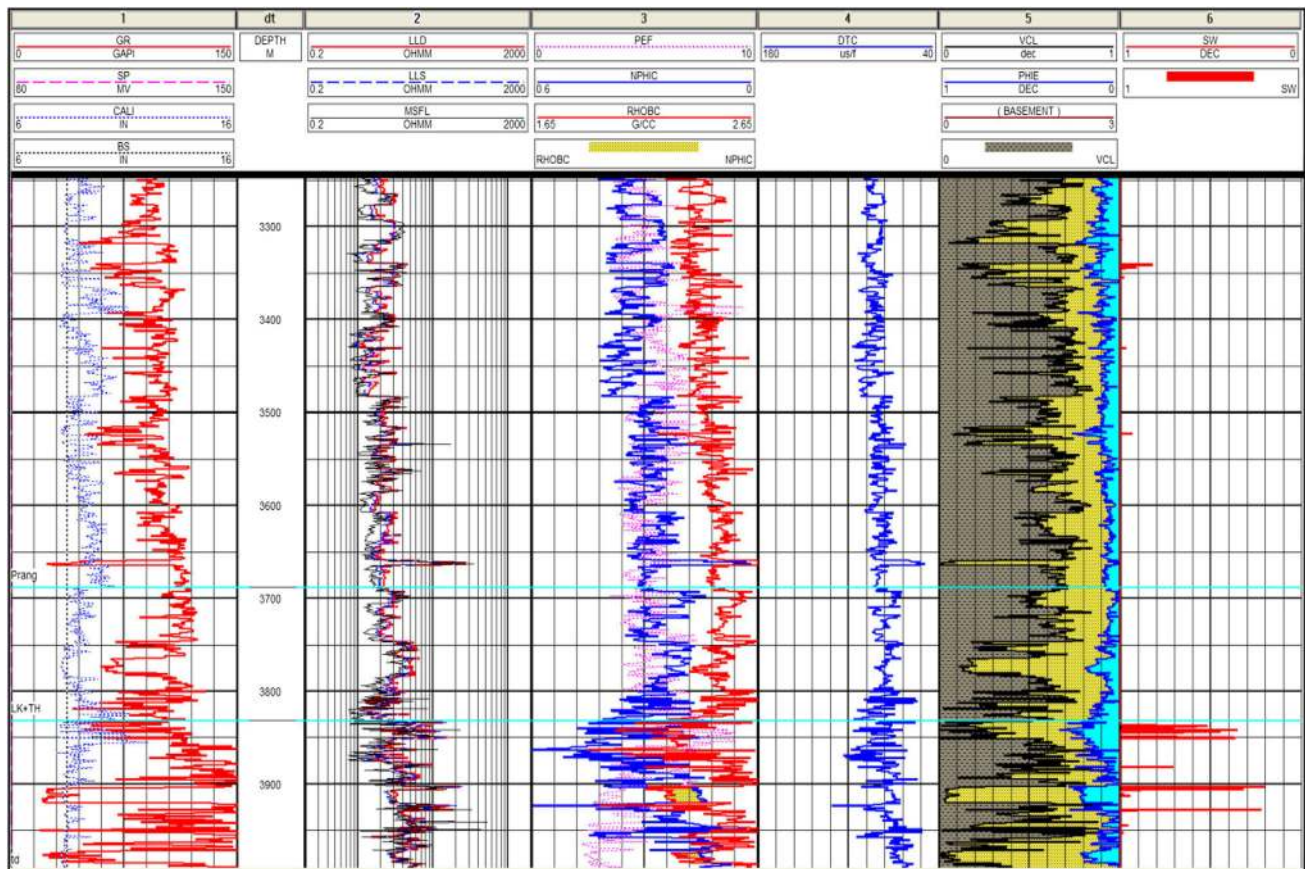

Fig. 16 Petrophysical results of one representative well-A

Mineral mixing

The minerals and pore spaces are mixed using the self-consistent method (Berryman 1980). In Berryman self-consistent method, the pore space is modeled as ellipsoids with an assigned aspect ratio which is dependent on the mineral with which the pore space is associated. The minerals are also modeled as ellipsoids and assigned the same aspect ratio as their associated pores. The rock/fluid properties which are used to model the sand shale sequences using the self-consistent method are summarized in Table 4.

Fluid mixing

The fluids, brine and hydrocarbon are mixed to produce effective properties that can be used in Gassmann modeling. The density mix is straightforward using the volume

Table 4 Rock properties for different lithology and fluid used to model the sand/shale sequences

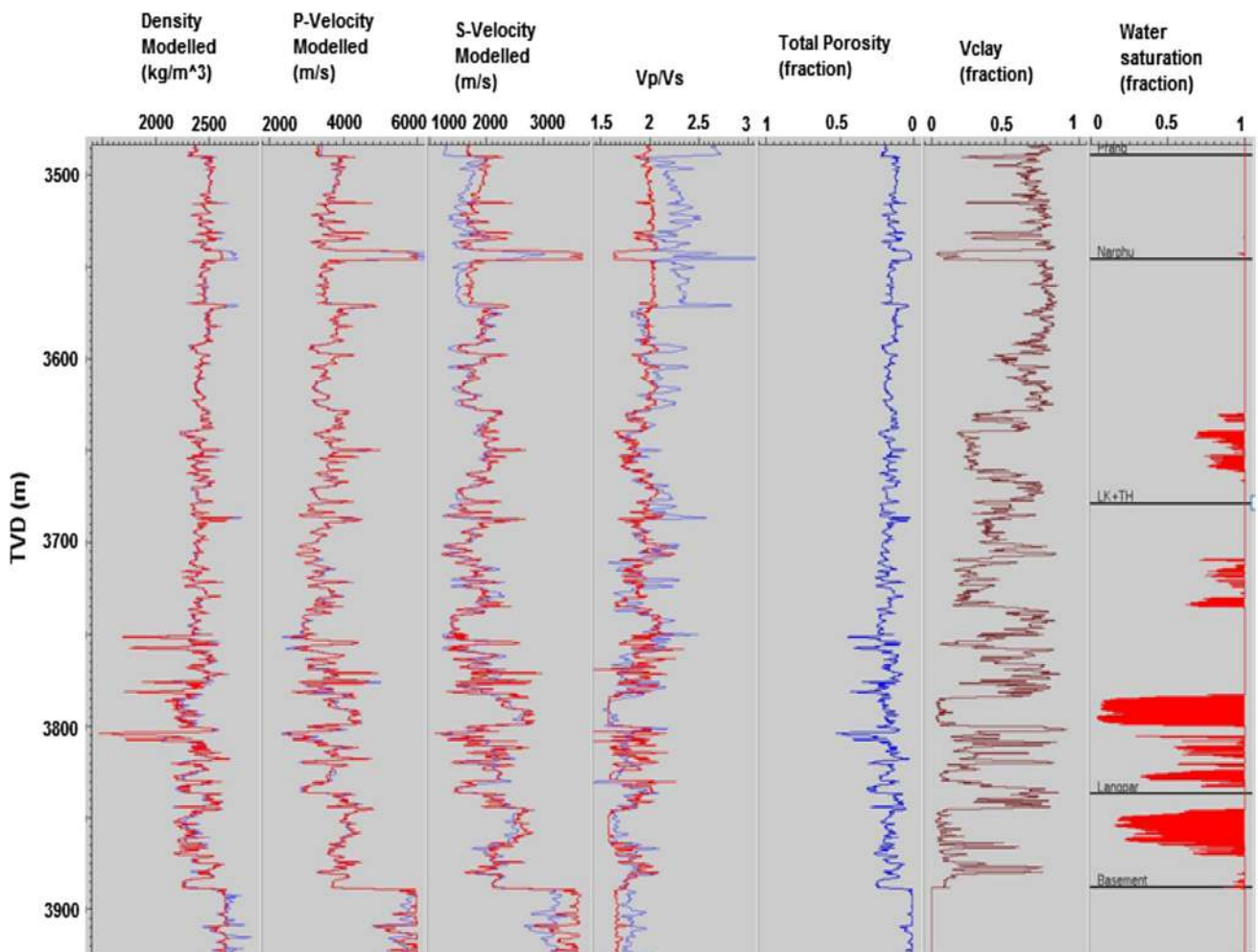|	Density (kg/m³)	P-velocity (m/s)	S-velocity (m/s)	Aspect ratio
Grain	2650	6200	3800	Varied with porosity
Dry clay	Varied with depth	Varied with depth	Varied with depth	Varied with porosity
Brine	1109	1691.5	n/a	
Gas	220	591	n/a	
Live oil	776	1037	n/a	

Fig. 17 A comparison of rock physics modeled log with measured log for one representative well-A

average of the densities of different fluids present. The acoustic properties are mixed using Brie's formula (Brie et al. 1995) to account for the variation in distribution of the different fluids within the pore space,

$$k_{fl} = (k_{br} - k_g)S_w^e + k_g \qquad (7)$$

where k_{fi} is the effective acoustic modulus of the fluid mixture, k_{br} is the acoustic modulus of brine, k_g is the acoustic modulus of gas (or oil) and S_w is the brine saturation. The exponent 'e' can vary from 1 to infinity, where

1 represents a complete mixing of the fluids. A value of e = 3 is mainly used in the current modeling.

Mineral and fluid mixing

Gassmann (1951a, b) equation is used to model the effect of the fluids in the pore spaces (Biot 1956). The fluids are initially incorporated with the mixture that represents saturations in the invaded zones as seen by the log. Various versions of the fluid substituted logs (all brine, all gas, and

Fig. 18 Measured P-impedance versus modeled V_P/V_S cross-plots for all wells colored by Litholog
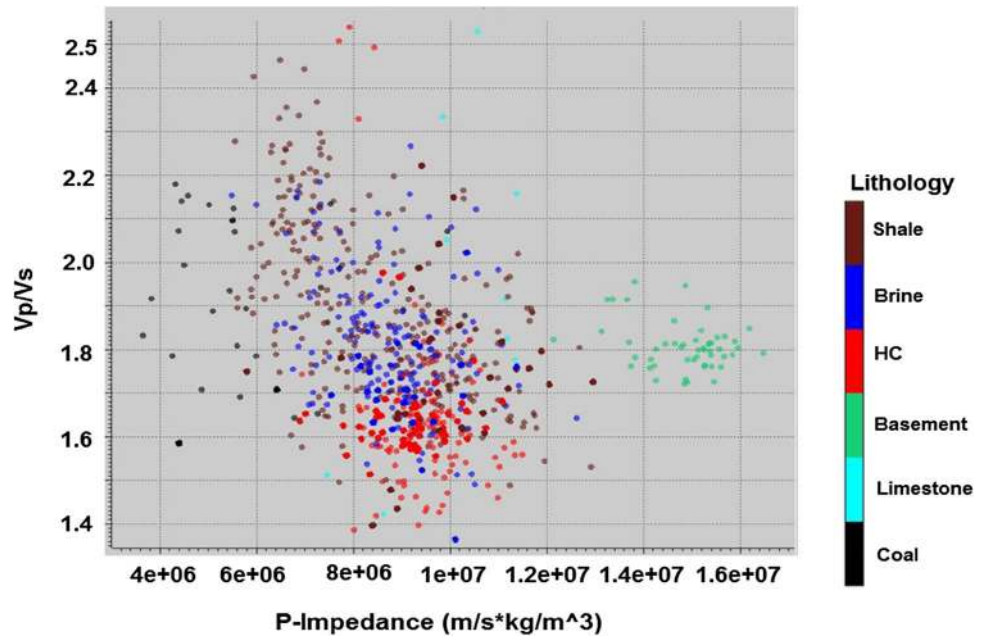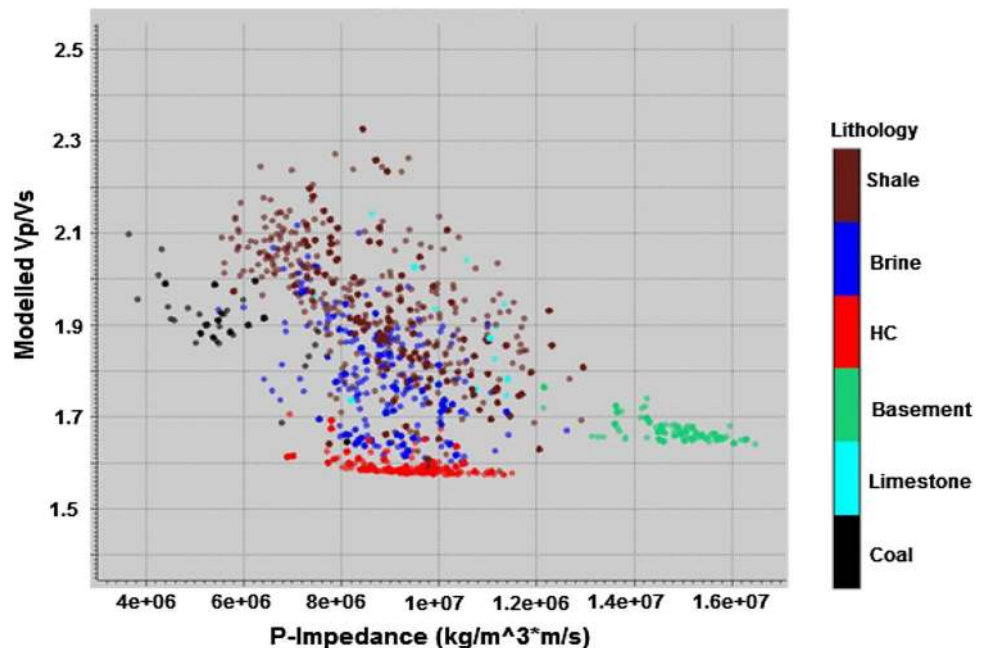

Fig. 19 Measured P-impedance versus modeled V_P/V_S for all wells colored by Litholog

all oil) are generated. The quality of the model is assessed by comparing the modeled and measured log data as shown in Fig. 17. In Fig. 17, the modeled density, P-velocity, S-velocity and V_P/V_S colored in red are plotted in the first four tracks on top of the measured curves colored in blue. Track 5, 6 and 7 represent total porosity, V_{clay} and S_w. The plots indicate that there is good correlation between the modeled logs and measured logs data. However, the modeled S-sonic log shows some deviations with the

measured log data at several places because measured S-sonic log is affected by bore hole caving which might have caused abrupt variations in the log. There are some spikes and missing data observed in the measured logs which have also been taken care of by the rock physics model. The model could also rectify the sonic data where the measured data may have not been processed properly.

The final modeled elastic logs also allow one to understand the relationship between the petrophysical and

Fig. 20 Measured P-impedance versus effective porosity for all wells colored by Litholog
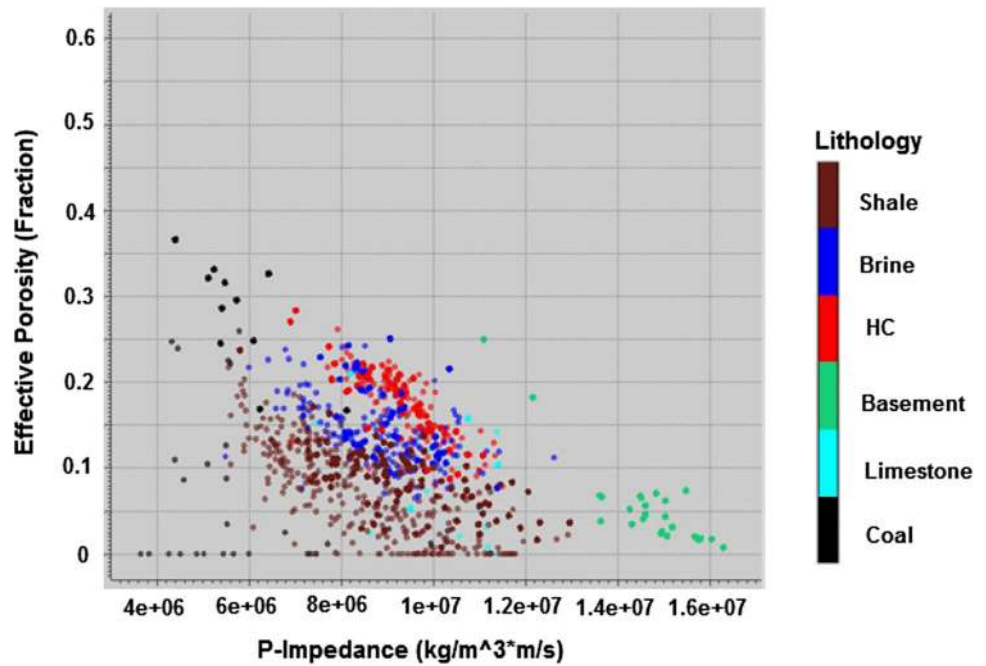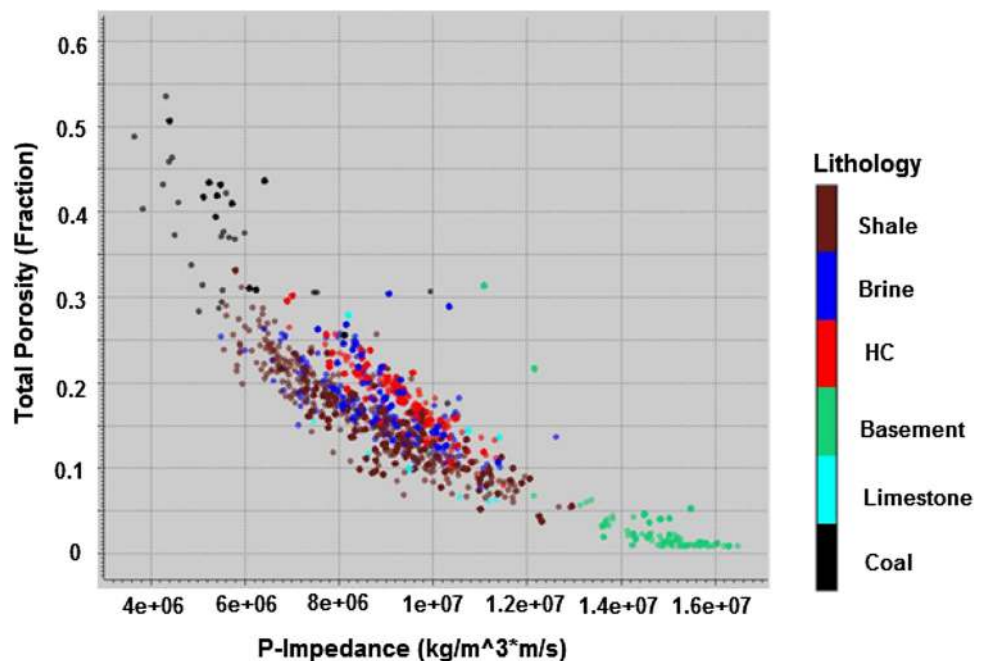
Fig. 21 Measured P-impedance versus total porosity for all the wells colored by Litholog

elastic rock properties which can be used further to predict the reservoir properties away from the well locations. Figures 18 and 19 show cross-plots of measured and modeled P-impedance versus V_P/V_S colored by Lithologs for all the wells, respectively. Some of the relations of the reservoir properties are tested by cross-plotting P-impedance versus effective and total porosity, P-impedance versus density as shown in Figs. 20, 21 and 22. Different Lithologies, e.g. shale, hydrocarbon, coal, and basement etc., show good separation of properties in P-impedance versus V_P/V_S domain.

Figures 18, 19, 20, 21 and 22 show that the rock physics-synthesized logs have preserved the separation of shale from non shale components, background shale trend, separation of the hydrocarbon samples, porosity trend for different lithology and the density information for different lithology. The resultant model explains the general behavior of the rock. The compaction trend is clearly seen in the density and P-sonic log (Fig. 23) which is responsible for an increase in P-impedance and a decrease in V_P/V_S with depth. Sands in general have higher P-impedance value than the surrounding shale. However, with the

Fig. 22 Measured P-impedance versus measured density for all the wells colored by Litholog
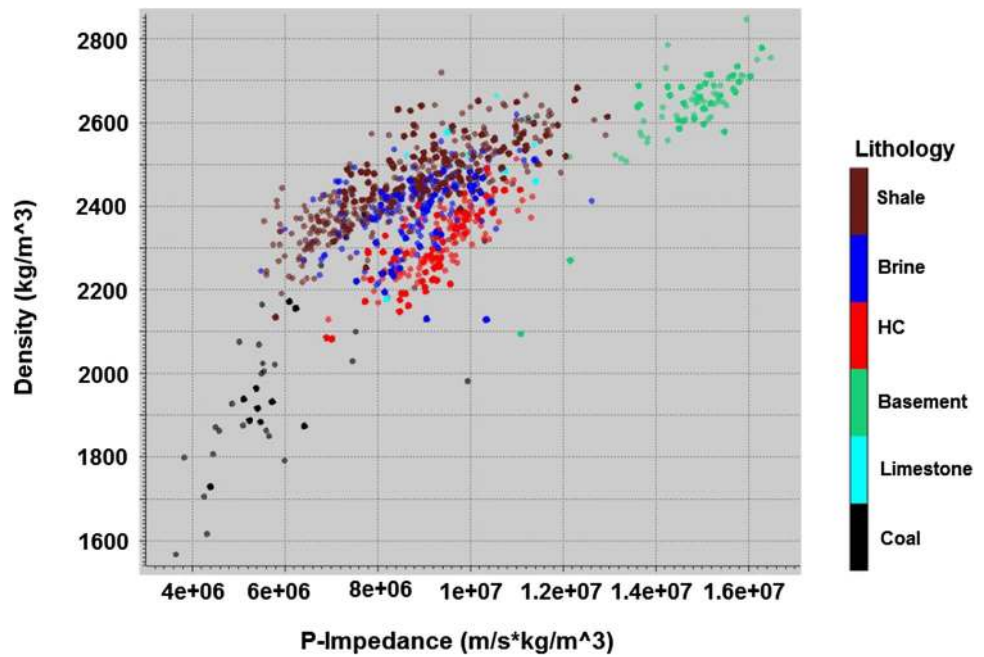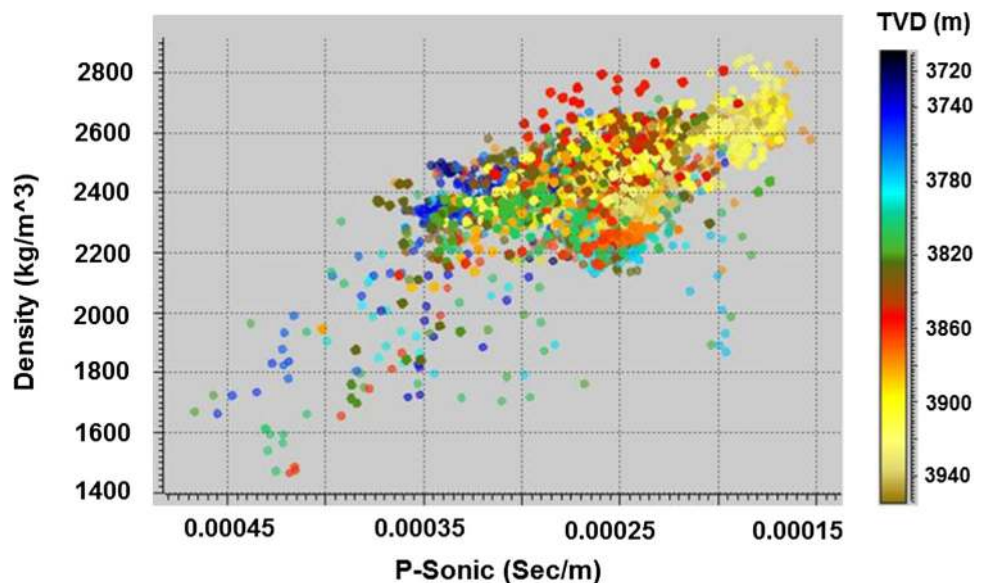

Fig. 23 Compaction trend in density and P-sonic logs cross-plot colored by depth

introduction of hydrocarbon, the impedance value decreases as expected.

Conclusions

A detailed petrophysical analysis blended with rock physics modeling have been carried out for reservoir characterization of Chandmari oilfield in Upper Assam-Arakan basin, India, using a suite of well log data from six wells in the field. Lithological interpretation and effects of rock minerals and fluids have been assessed. The Eocene reservoirs are mainly sandstone with inferred clay matrix up to 20% and some calcareous cementation. Some of these reservoirs are very clean with clay content as low as 5–10%. Sands are interpreted to be continuous in most of the blocks. However, there is some shale intercalations observed in many cases. A wide range of variation is found in water saturation with lowest value observed at 5%. The effective porosity for these sands is varying in the range of 15–22% for most of the wells. The effect of gas in the reservoir sands are very well understood in the log response for most of the wells. Gas bearing zone showed very big cross over for neutron-density curves and is also supported by very high resistivity. However, it was difficult to differentiate between oil and gas on the basis of the measured logs.

Rock physics modeled elastic logs also allowed to understand the relationship between the petrophysical and elastic rock properties to be used for further prediction of reservoir properties away from the well locations. The model explained the general behavior of the rock and synthesizes the good quality P-sonic and S-sonic logs where no recorded sonic data were available. Rock physics-synthesized logs also preserved the porosity trend and density information for different lithology. The compaction trend is clearly seen in the density and P-sonic log which causes an increase in P-impedance and decrease in V_P/V_S with depth.

References

Avseth P, Mukerji T, Mavko G (2005) Quantitative seismic interpretation: applying rock physics to reduce interpretation risk. Cambridge University Press, Cambridge, p 359

Avseth P, Mukherji T, Mavko G (2006) Quantitative seismic interpretation. Cambridge University Press, Cambridge

Balan KC, Banerjee B, Pati LN, Shilpkar KB, Pandey MN, Sinha MK, Zutshi PI (1997) Quantitative genetic modeling of Upper Assam Shelf. In: Proceedings of second international petroleum conference and exhibition, PETROTECH-97, New Delhi, vol 1, pp 341–349

Bateman RM (1985) Open-hole log analysis and formation evaluation Schlumberger Inc. In: Log interpretation principles. Schlumberger education services, Houston, USA

Batzle ML, Wang ZJ (1992) Seismic properties of pore fluids. Geophysics 57:1396–1408

Berryman JG (1980) Long-wavelength propagation in composite elastic media II ellipsoidal inclusions. J Acoust Soc Am 68:1820–1831

Berryman JG (1999) Origin of Gassmann's equations. Geophysics 64:1627–1629

Biot MA (1956) Theory of propagation of elastic waves in a fluid-saturated porous solid. J Acoust Soc Am 28:168–191

Brie A, Pampuri F, Marsala AF, Meazza O (1995) Shear sonic interpretation in gas-bearing sands. Soc Pet Explor (SPE) 30595:701–710

Chang HC, Kopaska-Merkel DC, Chen HC (2002) Identification of lithofacies using Kohonen self organizing maps. Comput Geosci 28:223–229

Datta Gupta S, Chatterjee R, Farooqui MY (2012) Rock physics template (RPT) analysis of well logs and seismic data for lithology and fluid classification in Cambay basin. Int J Earth Sci 101(5):1407–1426

Dresser A (1981) Well logging and interpretation techniques. Dresser Industries Inc., Addison

Ellis DV (1987) Well logging for earth scientists. Elsevier, New York

Gassmann F (1951a) Elastic waves through a packing of spheres. Geophysics 16:673–685

Gassmann F (1951b) Elasticity of porous media. Uberdie elastizitat-porosermedien, Vierteljahrsschrift der NaturforschendenGesselschaft 96:1–23

Gaymard R, Poupon A (1968) Response of neutron and formation density logs in hydrocarbon bearing formations. Log Anal 9(5):3–12

Gray D, Day S, Schapper S (2015) Rock physics driven seismic data processing for the Athabasca oil sands, Northeastern Alberta. CSEG Recorder March, pp 32–40

Han D, Batzle ML (2004) Gassmann's equation and fluid-saturation effects on seismic velocities. Geophysics 69:398–405

Inichinbia S, Sule PO, Ahmed AL, Hamaza H, Lawal KM (2014) Petro physical analysis of among hydrocarbon field fluid and lithofacies using well log data. IOSR J Appl Geol Geophys 2:86–96

Ishwar NB, Bhardwaj A (2013) Petrophysical well log analysis for hydrocarbon exploration in parts of Assam-Arakan basin, India. In: 10th Biennial international conference and exposition, society of exploration geophysicists, Kochi, India, p 153

Joshi GK, Shyammohan V, Reddy AS, Singh B, Chandra M (2004) Reservoir characterization through log property mapping in Geleki field of upper Assam, India. In: 5th Conference and exposition on petroleum geophysics, Hyderabad, India, pp 685–687

Mandal KL, Dasgupta R (2013) Upper Assam basin and its basinal depositional history. In: 10th Biennial international conference and exposition, society of petroleum geophysicists, Kochi, p 292

Mavko G, Mukerji T (1995) Seismic pore space compressibility and Gassmann's relation. Geophysics 60(6):1743–1749

Mavko G, Mukerji T, Dvorkin J (1998) The rock physics handbook: tools for seismic analysis of porous media. Cambridge University Press, Cambridge

Mukerji T, Avseth P, Mavko G, Takahashi I, González EF (2001) Statistical rock physics: combining rock physics, information theory, and geostatistics to reduce uncertainty in seismic reservoir characterization. Lead Edge 20(3):313–319. doi:10.1190/1.1438938

Naidu BD, Panda BK (1997) Regional source rock mapping in Upper Assam Shelf. In: Proceedings of the second international petroleum conference and exhibition (PETROTECH-97), New Delhi, vol 1, pp 350–364

Neog PK, Borah NM (2000) Reservoir characterization through well test analysis assists in reservoir simulation—a case study. In: SPE Asia Pacific oil and gas conference and exhibition, Brisbane, Australia, 16–18 October

Poupon A, Leveaux J (1971) Evaluation of water saturations in shaly formations. Log Anal 12(4):3–8

Rider M (1996) The geological interpretation of well log, 2nd edn. Whittles Publishing, London. ISBN-13: 978-0954190606

Sarasty JJ, Stewart RR (2003) Analysis of well-log data from the White Rose oilfield, offshore Newfoundland. CREWES Res Rep 15:1–16

Schlumberger (1967) Well evaluation conference Middle East, vol 1, Text vol 2, Examples 2. Schlumberger, Paris, France

Wandrey CJ (2004) Sylhet-Kopili/Barail-Tipam composite total petroleum system, Assam geological province, India. USGS Open File Report 2208-D

Xin G, Han D (2009) Lithology and fluid differentiation using rock physics templates. Lead Edge 28:60–65